FINITE ELEMENT COMPARISON OF DESIGN METHODS FOR LOCALLY SLENDER STEEL BEAMS AND COLUMNS

M. Seif[1] and B.W. Schafer[2]

ABSTRACT

The objective of this paper is to describe and analyze a series of nonlinear finite element analyses used to compare three design methods for locally slender, braced, steel beams and columns. The three design methods are: (i) the hot-rolled steel AISC Specification, (ii) the cold-formed steel AISI Specification which uses the effective width method throughout, and (iii) the cold-formed steel Direct Strength Method which was recently adopted as an alternative design method in the AISI Specification. To aid the comparison of the available methods the design strength formulas, for locally slender W-section beams and columns, are provided in a common notation. The resulting design expressions highlight the prominent role of elastic cross-section stability as the key parameter for strength prediction. The comparison for beams shows that the AISC and AISI methods take very different approaches to predicting the strength of locally slender sections. A nonlinear finite element analysis parameter study, using ABAQUS, is initiated for the purpose of understanding and highlighting the parameters that lead to the divergence between the capacity predictions of the different design methods. Particular attention is placed on understanding the regimes where the AISC methods give divergent results, from either the other Specifications, or the nonlinear finite element analysis results.

---

[1] Graduate Research Asst., Johns Hopkins University, mina.seif@jhu.edu

[2] Associate Professor, Johns Hopkins University, schafer@jhu.edu

INTRODUCTION

Typically, locally slender (noncompact or slender) cross-sections are avoided in design of hot-rolled steel structural members. However, this strategy becomes inefficient with the advent of high and ultra-high yield strength steels, as the increased yield stress drives even standard shapes from locally compact to locally slender. The effect of increasing the yield strength on local buckling is a topic that has seen some study in recent years (see e.g., Earls 1999). Initial analysis of the AISC provisions (Schafer and Seif 2008) indicates geometric regions where the existing AISC design approach may be excessively overly conservative, and other regions where it may be moderately unconservative. Efficient and reliable strength predictions are needed for hot-rolled steel cross-sections to take advantage of more locally slender sections. Since the design of locally slender cross-sections is common practice in cold-formed steel, the two design methods in current use for cold-formed steel are compared with the AISC approach herein.

DESIGN METHODS

The design of locally slender steel cross-sections may be completed by a variety of methods, three of which are examined here: (1) The AISC method, as embodied in the 2005 AISC Specification, labeled **AISC** herein, (2) The AISI Effective Width Method from the main body of the 2007 AISI Specification for cold-formed steel, labeled **AISI** herein, and, (3) The Direct Strength Method as given in Appendix 1 of the 2007 AISI Specification, labeled **DSM** herein.

For each of these three design methods the expressions for strength prediction of braced columns and beams have been provided in a common notation in Table 1 and Table 2, respectively. Previous work provided and examined the design expressions for unbraced columns with locally slender cross-sections (Schafer and Seif 2008). In this paper the design expressions for both columns and beams are provided, but only for the braced case, as this provides a focus on the local buckling strength predictions alone, and may be readily compared to the subsequently conducted nonlinear finite element analysis.

Table 1 Braced column strength for locally slender I-shaped section

AISC

$$P_n = Q_s Q_a A_g f_y$$

$$Q_s = \begin{cases} 1.0 & \text{if } f_{crb} \geq 2 f_y \\ 1.415 - 0.59\sqrt{\frac{f_{crb}}{f_y}} & \text{if } \frac{3}{5} f_y < f_{crb} < 2 f_y \\ 1.1\frac{f_{crb}}{f_y} & \text{if } f_{crb} \leq \frac{3}{5} f_y \end{cases}$$

$$Q_a = \begin{cases} 1.0 & \text{if } f_{crh} > 2 f \\ 1 - \left(1 - 0.9\sqrt{\frac{f_{crh}}{f_y}}\left(1 - 0.16\sqrt{\frac{f_{crh}}{f_y}}\right)\right)\frac{ht_w}{A_g} & \text{if } f_{crh} \leq 2 f \end{cases}$$

$$f = Q_s f_y$$

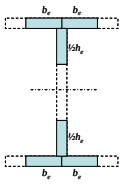

AISI (Effective Width Method)

$$P_n = A_{eff} f_y$$

$$A_{eff} = 4 b_e t_f + h_e t_w$$

$$b_e = \rho_b b \text{ where } \rho_b = \begin{cases} 1 & \text{if } f_{crb} \geq 2.2 f_y \\ \left(1 - 0.22\sqrt{\frac{f_{crb}}{f_y}}\right)\sqrt{\frac{f_{crb}}{f_y}} & \text{if } f_{crb} < 2.2 f_y \end{cases}$$

$$h_e = \rho_h h \text{ where } \rho_h = \begin{cases} 1 & \text{if } f_{crh} \geq 2.2 f_y \\ \left(1 - 0.22\sqrt{\frac{f_{crh}}{f_y}}\right)\sqrt{\frac{f_{crh}}{f_y}} & \text{if } f_{crh} < 2.2 f_y \end{cases}$$

DSM (Direct Strength Method, AISI Appendix 1)

$$P_n = \begin{cases} P_y & \text{if } P_{cr\ell} \geq 1.66 P_y \\ \left(1 - 0.15\left(\frac{P_{cr\ell}}{P_y}\right)^{0.4}\right)\left(\frac{P_{cr\ell}}{P_y}\right)^{0.4} P_y & \text{if } P_{cr\ell} < 1.66 P_y \end{cases}$$

$$P_y = A_g f_y$$

$$P_{cr\ell} = A_g f_{cr\ell}$$

Table 2 Braced beam strength for locally slender I-section

AISC

$M_n = \min\left(M_{nw}, M_{nf}\right)$

WLB $M_{crh} \geq 2.3M_y$ $\quad M_{nw} = M_p$

$2.3M_y > M_{crh} > M_y$ $\quad M_{nw} = M_p - \left(M_p - 0.7M_y\right)\dfrac{\sqrt{M_y / M_{crh}} - 0.66}{1 - 0.66}$

$M_y \geq M_{crh}$ $\quad M_{nw} = R_{pg} M_y$

$R_{pg} = 1 - \dfrac{a_w}{1200 + 300a_w} 5.7\sqrt{\dfrac{E}{F_y}}\left(\sqrt{M_y / M_{crh}} - 1\right) \leq 1$

$a_w = ht_w / b_f t_f = A_{web} / A_{flange} \leq 10$

FLB $M_{crb} \geq 6.9M_y$ $\quad M_{nf} = M_p$

$6.9M_y > M_{crb} > M_y$ $\quad M_{nf} = M_{nw} - \left(M_{nw} - 0.7M_{y*}\right)\dfrac{\sqrt{M_y / M_{crb}} - 0.38}{1.0 - 0.38}$

$M_{y*} = M_y$ if $M_{crh} \geq M_y$ else $M_{y*} = M_{nw}$

$M_y \geq M_{crb}$ $\quad M_{nf} = M_{crb} = S_x f_{crb}$

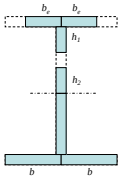

AISI (Effective Width Method)

$M_n = S_{eff} f_y$

$S_{eff} = I_{eff} / y_{eff}$, $I_{eff} = \int_{eff} y^2 dA$, $y_{eff} = \int_{eff} y dA / \int_{eff} dA$

$$b_e = \rho_b b \text{ where } \rho_b = \begin{cases} 1 & \text{if } f_{crb} \geq 2.2 f_y \\ \left(1 - 0.22\sqrt{\dfrac{f_{crb}}{f_y}}\right)\sqrt{\dfrac{f_{crb}}{f_y}} & \text{if } f_{crb} < 2.2 f_y \end{cases}$$

$$h_e = \rho_h h \text{ where } \rho_h = \begin{cases} 1 & \text{if } f_{crh} \geq 2.2 f_y \\ \left(1 - 0.22\sqrt{\dfrac{f_{crh}}{f_y}}\right)\sqrt{\dfrac{f_{crh}}{f_y}} & \text{if } f_{crh} < 2.2 f_y \end{cases}$$

$h_1 = h_e / 4$, $h_2 = h_e / 4$, for $h / b \geq 4$

DSM (Direct Strength Method – AISI Appendix 1)

$M_{cr\ell} > 1.66M_y$ $\quad M_n = M_p - \left(M_p - M_y\right)\left(1 - 1.66\sqrt{\dfrac{M_{cr\ell}}{M_y}}\right)$

$M_{cr\ell} \leq 1.66M_y$ $\quad M_n = \left(1 - 0.15\left(\dfrac{M_{cr\ell}}{M_y}\right)^{0.4}\right)\left(\dfrac{M_{cr\ell}}{M_y}\right)^{0.4} M_y$

Table notes:
Expressions have been limited to centerline models of an I-shaped section. In practice AISC and AISI use slightly different k values to determine f_{crb} and f_{crh}, in the parametric studies herein they are set equal. For columns k_f=0.7 and k_w=5.0, for beams k_f employs the AISC expression :

$$M_{crb} = S_x f_{crb} = S_x k_f \frac{\pi^2 E}{12\left(1-\nu^2\right)}\left(\frac{t_f}{b}\right)^2,\ 0.35 \le k_f = \frac{4}{\sqrt{h/t_w}} \le 0.76$$

while k_w=36 (refer to Seif and Schafer 2009a for a more detailed discussion on the local plate buckling coefficients values underlining the AISC specification). For DSM $f_{cr\ell}$ or $M_{cr\ell}$ are determined from an elastic bucking finite strip analysis (Schafer and Ádány 2006). For AISI (Effective Width) the neutral axis shift has been ignored, for the studied sections the error is small. The DSM expression for $M_{cr\ell}$>1.66M_y is based on recent work (Shifferaw and Schafer 2008) and is under ballot at AISI at the time of this writing.

The column design equations of Table 1 have been previously detailed (Schafer and Seif 2008), summary observations follow: (a) local plate buckling (f_{crh}, f_{crb}, $f_{cr\ell}$) and yield stress (f_y) are the key parameters for determining the strength, regardless of the method; (b) AISC and AISI-Effective Width use local plate buckling solutions for the isolated flange (f_{crh}) and web (f_{crb}), while DSM uses the local bucking solution for the cross-section as a whole ($f_{cr\ell}$); (c) AISC ignores post-buckling capacity in slender unstiffened elements (see the Q_s expression).

The beam design equations of Table 2 provide the strength prediction for laterally braced I-shaped cross-sections which may be locally slender. Even a cursory examination of Table 2 reveals that AISC, AISI, and DSM use radically different methods to provide the strength prediction of locally slender beams. The AISC method is compiled from sections F2-F5 of the Specification (also see White 2008). Similar to Schafer and Seif (2008) for columns, the λ limits (h/t_w, $b_f/2t_f$) have been replaced by f_{crh} and f_{crb} limits (actually M_{cr} limits where M_{cr} is just $S_x f_{cr}$) as (a) this is more general, (b) this allows for a comparison between different design methods in a common notation, and (c) the centrality of elastic local buckling is made clear by this change.

As the primary audience for this paper is engineers familiar with the AISC Specification, some additional attention to the AISC approach is provided here. Compilation of the AISC Specification from sections F2-F5 is non-trivial. However, it is possible to divorce the web local buckling limit state and flange local bucking limit state from the individual F2-F5 sections. For the convenience of users of the AISC Specification, these expressions are provided in notation similar to AISC in the following (also this makes clear the λ to M_{cr} conversions used and provided in Table 2). M_n is the minimum of $M_{n\ell w}$ and $M_{n\ell f}$.

AISC Web local buckling

C: $\lambda_w \le \lambda_{pw}$ then $M_{n\ell w} = M_p$

NC: $\lambda_{pw} < \lambda_w < \lambda_{rw}$ then $M_{n\ell w} = M_p - \left(M_p - M_y\right)\dfrac{\lambda_w - \lambda_{pw}}{\lambda_{rw} - \lambda_{pw}}$

S: $\lambda_{rw} \le \lambda_w$ then $M_{n\ell w} = R_{pg} M_y$

$$R_{pg} = 1 - \frac{a_w}{1200+300a_w}\left(\lambda_w - \lambda_{rw}\right) \le 1$$

$$a_w = ht_w / b_f t_f = A_{web} / A_{flange} \le 10$$

AISC Flange local buckling

C: $\lambda_f \le \lambda_{pf}$ then $M_{n\ell f} = M_p$

NC: $\lambda_{pf} < \lambda_f < \lambda_{rf}$ then $M_{n\ell f} = M_{n\ell w} - \left(M_{n\ell w} - 0.7M_{y*}\right)\dfrac{\lambda_f - \lambda_{pf}}{\lambda_{rf} - \lambda_{pf}}$

$M_{y*} = M_y$ if web NC or C $\lambda_w < \lambda_{rw}$

$M_{y*} = M_{n\ell w}$ if web S $\lambda_{rw} \le \lambda_w$

S: $\lambda_{rf} \le \lambda_f$ then $M_{n\ell f} = M_{cr\ell f}$

where λ's are defined in Table B4.1 of AISC, and $M_{cr\ell f}$ is the local buckling of the flange, i.e., $S_x f_{cr}$, and the k for f_{cr} is defined in terms of h/t_w, (see notes following Table 2).

FE PARAMETRIC STUDY

A nonlinear finite element (FE) analysis parameter study is initiated for the purpose of understanding and highlighting the parameters that lead to the divergence between the capacity predictions of the different design methods under axial and bending loads.

The FE analysis is conducted on stub (short) members, avoiding global (i.e., flexural, or lateral-torsional) buckling modes, and focusing on local buckling modes alone. The length of the studied members was determined according to the stub column definitions of SSRC (i.e., Galambos 1998). Based on the authors judgment, AISC W14 and W36 sections are selected for the study as representing "common" sections for columns and beams in high-rise buildings. The W14x233 section is approximately the average dimensions for the W14 group and the W36x330 for the W36 group. All sections are modeled with globally pinned, warping fixed boundary conditions, and loaded via incremental displacement or rotation for the columns and beams respectively.

Geometric variation

To examine the impact of slenderness in the local buckling mode, and the impact of web-flange interaction in I-sections, four series of parametric studies are performed under axial and bending loading:

- **W14FI**: a **W14**x233 section with a modified **F**lange thickness, that varies **I**ndependently from all other dimensions,
- **W14FR**: a **W14**x233 section with variable **F**lange thickness, but the web thickness set so that the **R**atio of the flange-to-web thickness remains the same as the original W14x233,
- **W36FR**: a **W36**x330 section with variable **W**eb thickness, but the flange thickness set so that the **R**atio of the flange-to-web thickness remains the same as the original W36x330, and
- **W36WI**: a **W36**x330 section with a variable **W**eb thickness, that varies **I**ndependently from all other dimensions,

as summarized in Table 3 and Figure 1.

Table 3 Parametric study of W-sections

	$b_f/2t_f$	h/t_w	h/b_f	t_f/t_w
W14x233	4.62	13.35	0.90	1.61
W14FI	varied	fixed	fixed	varied
W14FR	varied	varied	fixed	fixed
W36x330	4.54	35.15	2.13	1.81
W36FR	varied	varied	fixed	fixed
W36WI	fixed	varied	fixed	varied

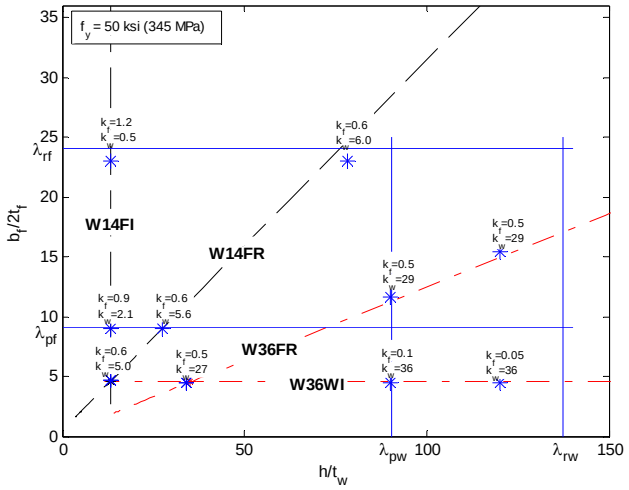

Figure 1 Variation of parameters as a function of h/t_w and $b_f/2t_f$ with back-calculated elastic buckling k values, and AISC λ limts for beams shown

For the purpose of this study, element thicknesses were varied between 0.05 in. (1.27 mm) and 3.0 in. (76.2 mm). While not strictly realistic, the values chosen here are for the purposes of comparing and exercising the design methods up to and through their extreme limits. Local slenderness may be understood as the square root of the ratio of the yield stress to the local buckling stress (i.e., $\sqrt{f_y/f_{cr}}$). The element local buckling stress is proportional to the square of the element thickness, thus the local slenderness is proportional to $1/t$. Here element thickness is varied and used as a proxy for investigating local slenderness, in the future, material property variations are also needed.

Mesh and element selection

Element choice and mesh refinement are key aspects of any finite element analysis. In structural steel research, where cross-section distortion and stability are of interest, researchers typically simplify the cross-section as a two-dimensional model at the cross-section mid-surface and employ shell finite elements to discretise the web and

flanges. ABAQUS, which is a widely used finite element analysis package, provides an element library that contains a wide range of different two-dimensional shell elements. For hot-rolled structural steel sections, typically the S4 or S4R elements are employed (with some debate between the two existing in the research community).

The S4 element has six degrees of freedom per node, adopts bilinear interpolation for the displacement and rotation fields, incorporates finite membrane strains, and its shear stiffness is yielded by "full" integration. The S4R element is similar to the S4 element, except that it obtains the shear stiffness by "reduced" integration. Researchers agree that models with S4 elements are stiffer and and sustain higher loads than identical meshes with S4R elements. Some, e.g. Dinis and Camotim (2006) attribute this to an "artificial" under-estimation of the member shear stiffness in the S4R element, others, e.g. Earls (2001), focus on the fact that the S4 element, which is fully integrated, should yield the correct solution if the mesh is properly refined to avoid shear locking. However, Earls found that even in reasonably refined meshes the S4 lead to longer run times than the S4R, and overly stiff results when compared with experiments.

To assess and compare the different shell elements, an elastic buckling analysis was performed on a W14X233 column with a length of 120 in. (3048 mm). Element type, including solid and shell elements were considered, along with mesh density, solver, and consideration of the k-zone. Key results are summarized in Table 4, see Seif and Schafer (2008) for full results.

Table 4 Results of element and mesh sensitivity study for W14x233 column

Model	**Solid**			**Shell**				
Element	S3D8R			S4	S4R	S4	S4R	S9R5
Solver	Subspace	Subspace	Lanczos	Subspace				
details	(no-k zone)	(w/ k-zone)	(w/ k-zone)	(normal mesh)		(fine mesh)		(normal mesh)
Mode	P_{cr} (N)	% diff.	% diff.	% diff.	% diff.	% diff.	% diff.	% diff.
1	22144	0.1%	0.0%	0.1%	-0.8%	0.0%	-0.2%	-2.1%
2	42344	4.5%	4.5%	-1.2%	-0.5%	-2.2%	-2.1%	-2.4%
3	42371	4.6%	4.6%	0.4%	1.1%	-0.9%	-0.9%	-1.1%
4	44646	1.1%	1.1%	-2.0%	-1.2%	-2.6%	-2.4%	-4.1%
5	45345	4.3%	4.3%	-1.7%	-1.8%	-1.8%	-1.8%	-4.2%
6	46438	4.3%	4.3%	-1.8%	-1.2%	-2.9%	-2.8%	-3.2%
7	50780	4.5%	4.5%	-3.6%	-3.2%	-4.9%	-4.8%	-5.2%
8	51359	4.0%	4.0%	-1.3%	-0.5%	-2.3%	-2.1%	-2.4%
9	52942	6.3%	6.3%	-4.1%	-3.4%	-4.9%	-4.8%	-5.0%
10	53163	6.4%	6.4%	-3.4%	-2.6%	-4.5%	-4.3%	-4.3%
average of 1-10		4.0%	4.0%	-1.9%	-1.4%	-2.7%	-2.6%	-3.4%

The results, Table 4, indicate that at least for stability loads, the sensitivity to mesh is greater than to element type. Further, the shell models generally give lower elastic buckling loads than the solid model, even when the solid model is theoretically the same (no k-zone is included). Both the normal and fine mesh show nearly converged solutions between the S4 and S4R. Dinis and Camotim (2006) indicate that for short columns, where local buckling governs, the S4 and S4R elements converge, while for longer columns in flexural buckling, they give up to 20% different results. This was not observed in the cases studied here, where the global flexural buckling mode governed, and the difference was less than 1.0%.

Considering computational speed and accuracy it was decided that the "normal mesh" (see Figure 3, five elements across each flange outstand, ten across the web, and aspect ratio of 1) was adequate for this study. Further, influenced in large part by the very small difference for the first mode S4 solution, the S4 was chosen over the S4R for further studies.

Material modeling

The material model follows classical metal plasticity: von Mises yield criteria, associated flow, and isotropic hardening. The uniaxial σ-ε diagram is provided in Figure 2a, and is similar to that employed by Barth et al. (2005). The curve is converted to a true σ-ε curve for the ABAQUS analysis.

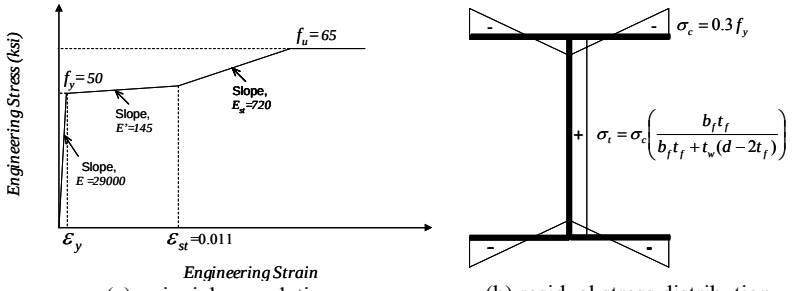

(a) uniaxial σ-ε relation (b) residual stress distribution

Figure 2 Idealized material model (a) σ-ε and (b) residual stresses

Residual stresses

Residual stresses form, primarily, due to differential cooling during manufacture. Szalai and Papp (2005) recently studied and compared commonly used residual stress distributions including: Young's parabolic distribution, the ECCS linear distribution, and Galambos and Ketter's constant linear distribution, as well as proposed a new distribution. For this work, the classic and commonly used distribution of Galambos and Ketter (1959), as shown in Figure 2b, is employed. Similar to other researchers (e.g., Jung and White 2006) the residual stresses are defined in the finite element analysis as initial longitudinal stresses, and given as the average value across the element at its center.

Geometric imperfections

Geometric imperfections have an important role to play in any collapse analysis involving stability. The focus of this study is on local buckling, where the specimens have been modeled at short length's such that global buckling (for the column or beam) does not influence the collapse response. Therefore, global imperfections: out-of-plumb-ness, out-of-straightness, etc. are ignored and only local imperfections are taken into consideration.

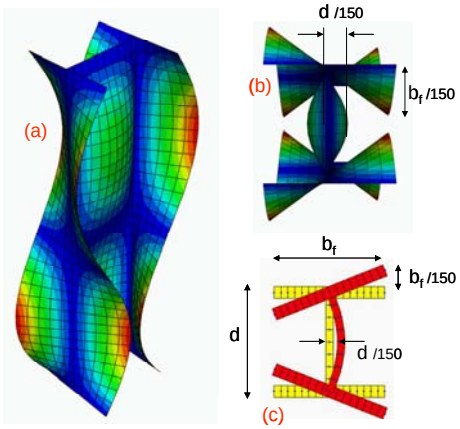

Figure 3 Typical column local buckling mode and initial geometric imperfections for the analysis (a) ABAQUS isometric, (b) ABAQUS front view, and (c) CUFSM front view, with scaling factor.

For the local imperfections it would be ideal to simulate actual expected imperfections, both in distribution and magnitude. However, information is limited and current practice tends to favor the use of manufacturing tolerances (ASTM A6/A6M-04b 2003) or similarly motivated rules of thumb. One such simple rule, commonly employed (see, e.g Kian and Lee 2002) is to introduce an initial web out of flatness of *d/150* and an initial tilt in the compression flanges of $b_f/150$. Similar magnitudes were adopted here, though additional work is needed.

For this study, the imperfections are defined by scaling the local buckling eigenmode from a previous buckling analysis. Buckling analysis was performed on the W14x233 and the W36x330. The first buckling mode, which is a local mode, is then introduced to the model as an initial geometric imperfection (the same mode for all the W14 and W36 parametric studies). The mode is scaled such that either the web out-of-flatness equals *d/150*, or tilt in the compression flange equals $b_f/150$. A typical local buckling mode for a column, and the imperfections used for its analysis, are provided in Figure 3.

RESULTS

As discussed previously (see Table 3 and Figure 1) the parametric study is broken into 4 groups: W14FI, W14FR, W36FR, and W36WI. Here the results of the parametric study are presented for each group, including comparisons to the AISC, AISI, and DSM design methods as summarized in Table 1 and Table 2. Due to limited space the results are condensed, see Seif and Schafer (2009b) for full results and discussion.

Columns

Typical load displacement results for the nonlinear FE collapse analysis of the stub column specimens are shown for the W36WI group in Figure 4. The thicker (recall t_w is varied here) specimens develop significant strain hardening (in compression!) while the thinner specimens exhibit less displacement before collapse. The peak loads recorded, denoted with a "*" in Figure 4, are in excess of the squash load ($P_y=A_g fy$) due to the strain hardening. For comparison of design methods, this strength was deemed unrealistic. As an alternative the peak load that was recorded at a displacement equal to 3 times the gross

yield displacement ($\Delta=3\Delta_y$, $\Delta_y=P_y/E$) denoted as a "o" in Figure 4 was utilized as the predicted strength (P_n). This same procedure was employed for all the parametric studies.

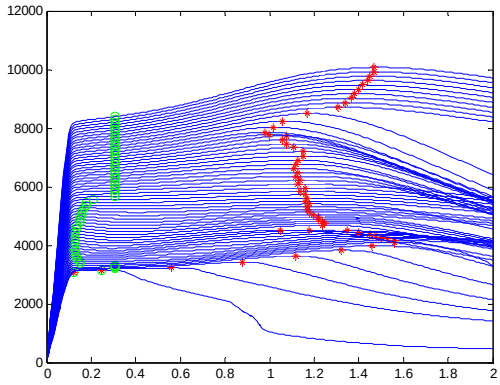

Figure 4 Load-displacement for W36WI column study

The ABAQUS predicted capacities are compared to the AISC, AISI, and DSM methods in Figure 5 and Figure 6. Figure 5 presents the results for each of the 4 parameter studies. Figure 6 presents all 4 studies against each of the design methods. The horizontal axis in all figures is the elastic local slenderness of the cross-section: $\sqrt{f_y/f_{cr\ell}}$. Where $f_{cr\ell}$ is determined for each cross-section from a finite strip analysis. Note, for an elastic buckling analysis $f_{crb}=f_{crh}= f_{cr\ell}$; however for AISC and AISI the strength prediction uses assumed k's to determine f_{crb} and f_{crh} thus $f_{crb}\neq f_{crh}\neq f_{cr\ell}$ for AISC and AISI. If AISC and AISI f_{crb} and f_{crh} are forced to the $f_{cr\ell}$ value, the strength predictions are changed – an example comparison for this case is provided in Figure 7 for the W14FI study.

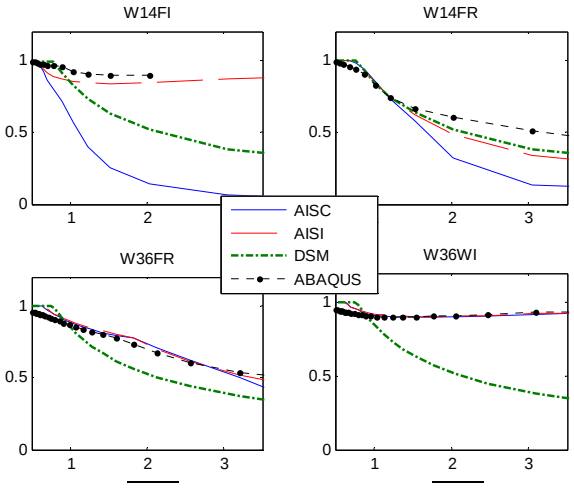

Figure 5 Results of column parametric study for 4 study groups

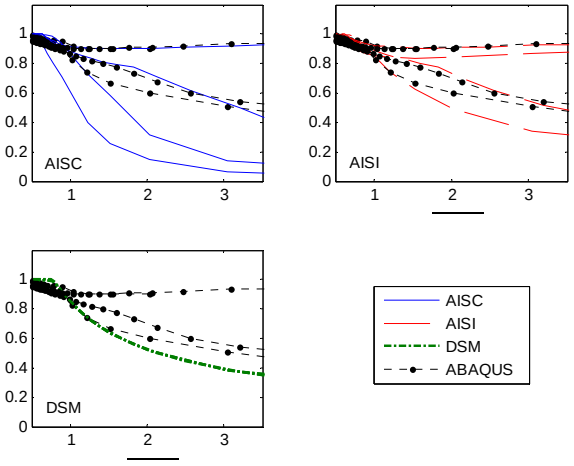

Figure 6 Results of column parametric study for 3 design methods

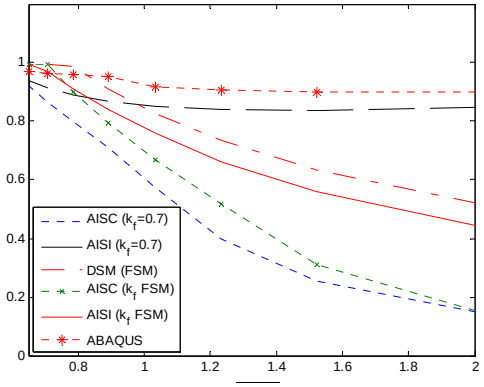

Figure 7 Column study results for W14FI considering alternative design methods where $f_{cr\ell}$ (from FSM) replaces f_{crb} and f_{crh} in AISC and AISI

Beams

The moment-rotation results for the W36WI parametric study of braced (short) beams is provided in Figure 8. The beams with the thinnest webs have a dramatic drop in moment-rotation response past their peak capacities, though nearly all studied beams develop the plastic capacity (which is largely a function of the flanges, a variable that is not changing in the W36WI study). Similar to columns, the rotation at $3\theta_y$ (where $\theta_y=M_yL/2EI$) was taken as a maximum allowable rotation, and the M_n at this value used as the predicted strength of the beams when comparing with design methods.

The predicted capacities from the nonlinear collapse analysis in ABAQUS are shown for each of the 4 parameter groups in Figure 9 and compared against the design methods directly in Figure 10. As for the beams, the local slenderness $\sqrt{f_y/f_{cr\ell}}$ (or equivalently $\sqrt{M_y/M_{cr\ell}}$) is used as the horizontal axis, while the vertical axis is the capacity normalized to the plastic moment, M_p.

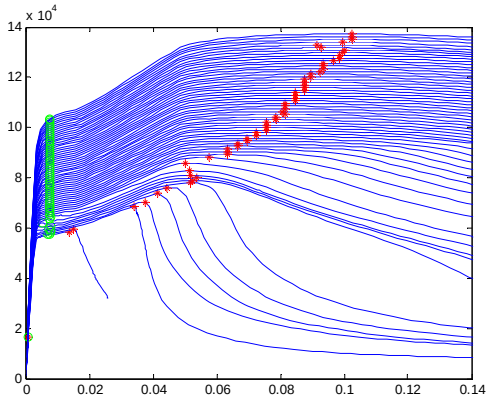

Figure 8 Moment-rotation for W36WI beam study

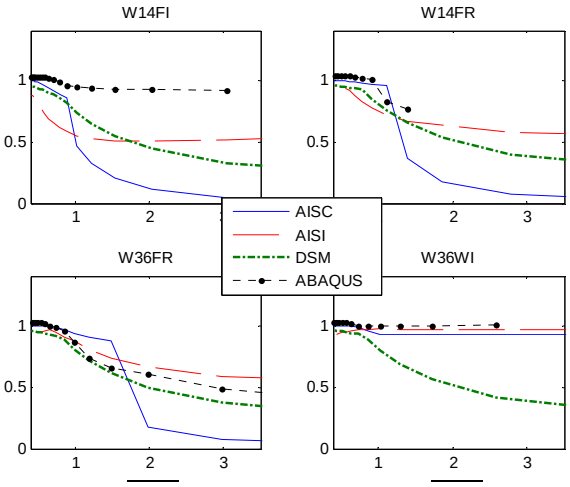

Figure 9 Results of beam parametric study for 4 study groups

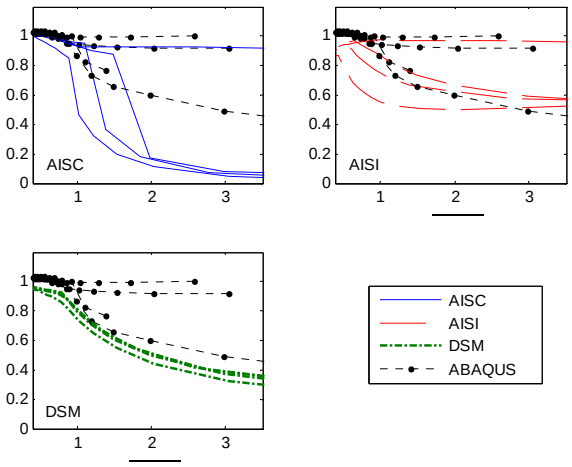

Figure 10 Results of beam parametric study for 3 design methods

DISCUSSION

The focus of the following discussion is the performance of the design methods in comparison with the capacities predicted by the nonlinear finite element analysis.

Columns

AISI's implementation of the Effective Width Method provides, by far, the best prediction of the column capacity. Only in the W14FR study does any method (DSM in this case) slightly outperform AISI.

AISC provides reliable predictions when the flange is non-slender; however AISC is unduly conservative whenever the flanges become slender (regardless of the web). The level of conservatism is large enough to make AISC design with slender flanges completely uneconomical.

DSM provides a reasonable approximation only when both the web and flange slenderness are changed – when one element is much more slender than another (for instance the flange in the W14FI study or the

web in the W36WI study) the DSM approach is overly conservative. For example, in the W36WI group, the presumption that the local buckling of the web initiates a similar local buckling in the flange does not occur. Examination of the deformed shape at collapse shows that the deformation is primarily one of web local buckling with little flange deformation. DSM's assumption, driven from elastic stability analysis, that member local buckling and member strength are one in the same is not observed in this section.

It is worth noting that this phenomenon (where DSM provides overly conservative predictions) exists in cold-formed steel members (which are of constant thickness) when one element is significantly wider than another. In these cases it has been found that although DSM is conservative, such sections also have significant serviceability problems. Such sections with highly varying element slenderness typically benefit from the inclusion of a longitudinal stiffener which provides a significant boost to the elastic buckling of the slender element and brings DSM predictions back in-line with observed capacities. Nonetheless, this phenomenon needs further study before DSM can be fully realized in structural steel.

Beams

AISC predictions are excellent when the section is compact. For noncompact flanges, AISC may be modestly unconservative (see W36FR, W14FR results), while for slender flanges, as in columns, the AISC predictions are excessively conservative. The web expressions appear to provide adequate strength predictions for all ranges (see W36WI results), again as long as the flange is compact. Transitions in the AISC expressions are not necessarily smooth (this is noted in the AISC commentary) and large disincentives, inconsistent with observed performance, are put on slender flanges.

AISI's Effective Width Method is for beams, like columns, the overall best performer in comparison with the FE results. However, unlike in columns when all cases agreed well, the W14FI study shows the effective width of the flange to be too conservative (presumably because beneficial stabilization by the compact web is not accounted

for). The W36 parameter study results are predicted quite well. Although AISI provides expressions for inelastic reserve (i.e., when $M_n > M_y$), the expressions involved and the solution are not in closed-form; therefore they have been ignored in Table 2 and the presented figures, and the AISI capacity is limited to M_y as shown.

DSM's accuracy for the beams meets or exceeds AISI and AISC except for the W36WI case, where the method is progressively more conservative as the web slenderness increases (see the discussion of DSM for columns above). Note, multiple curves are presented for DSM in Figure 10 because of the normalization to M_p (as opposed to M_y).

Overall

AISC's solutions are overly approximate for locally slender sections and deserve improvement, particularly for flanges (unstiffened elements). AISI's effective width, while the most complicated of the methods, appears to provide the most accurate solution, particularly for braced (stub) columns. The simplicity of DSM is obvious in the expressions and the curves, but the elastic web-flange interaction assumed in the method is not always realized. DSM provides a consistently conservative, and conceptually simple prediction method that is worthy of further study.

Future Work

The next step in this research is the extension of the parametric study to long columns and beams where the locally slender cross-sections may interact with global (flexural, lateral-torsional, etc.) buckling modes. Of particular interest is the interaction of sections such as in the W36WI study of Figure 8 where the sections predicted to have quite low capacities by DSM show the potential for much stronger interaction with global modes due to the abruptness of the moment-rotation response. The available design methods treat these local-global interactions with quite different approaches, and thus further study is needed in this regime. In addition, studying the sensitivity to additional input parameters: imperfections, residual stresses, and material stress-strain curve is needed. A primary goal of this research remains to provide recommendations for the extension of DSM to structural steel.

CONCLUSIONS

The design of locally slender steel cross-sections may be completed by a variety of methods. For braced (short) columns and beams, design expressions in common notation are provided for the AISC Specification, the AISI Specification (effective width method) and DSM the Direct Strength Method (as adopted in Appendix 1 of the AISI Specification as an alternative design procedure). The key parameters, found throughout all 3 design methods, are the elastic local (element, or member) buckling stress and the material yield stress. The design expressions indicate significantly different solution methodologies to this common problem, particularly for beams.

A parametric study of braced (short) columns and beams is conducted with nonlinear finite element models in ABAQUS, deformed to collapse, and compared with the AISC, AISI, and DSM design predictions. The parametric study focuses on W14 and W36 sections, where through modification of element thicknesses, the flange slenderness, and/or web slenderness are systematically varied (from compact, to noncompact, to slender in the parlance of AISC).

The results indicate that AISC is overly conservative when the flange is slender, AISC's assumption of little to no post-buckling reserve in unstiffened elements is not borne out by the analysis. AISI's effective width method is a reliable predictor, only for the beam studies does AISI provide overly conservative solutions when the web is compact but the flange slender. DSM provides reliable predictions when both the flange and web slenderness vary together, but is overly conservative when one element is significantly more slender than another. Additional work on long beams and columns with local-global interaction is underway.

ACKNOWLEDGMENTS

The authors of this paper gratefully acknowledge the financial support of the AISC, and the AISC Faculty Fellowship program in this research. Any views or opinions expressed in this paper are those of the authors.

DEFINITION OF KEY VARIABLES

A_g = gross cross-sectional area
b = half of the flange width (b_f=2b)
E = modulus of elasticity
f_{crb} = flange local buckling stress = $k_f[\pi^2 E/(12(1-\nu^2))](t_f/b)^2$
f_{crh} = web local buckling stress = $k_w[\pi^2 E/(12(1-\nu^2))](t_w/h)^2$
$f_{cr\ell}$ = cross-section local buckling stress, e.g. by finite strip
f_y = yield stress
h = centerline web height
k_f = flange plate buckling coefficient
M_{crb} = web local buckling moment = $S_x f_{crb}$
M_{crh} = flange local buckling moment = $S_x f_{crh}$
$M_{cr\ell}$ = cross-section local buckling moment = S_x $f_{cr\ell}$, e.g. by finite strip
M_n = nominal flexural capacity
M_p = plastic moment
M_y = moment at first yield
P_n = nominal compressive capacity
S_x -= gross section modulus about the x-axis
t_f = flange thickness
t_w = web thicknes
$\lambda_f = b/t_f$ also see AISC Table B4.1 for λ_{fr}, λ_{fp}
$\lambda_w = h/t_w$ also see AISC Table B4.1 for λ_{wr}, λ_{wp}
ν = Poisson's ratio

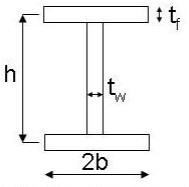

Sketch showing simplified section geometry

REFERENCES

AISC (2005). *"Specification for Structural Steel Buildings"*, American Institute of Steel Construction, Chicago, IL. ANSI/ASIC 360-05.

AISI (2007). "*North American Specification for the Design of Cold-Formed Steel Structures"*, Am. Iron and Steel Inst., Washington, D.C., AISI-S100.

ASTM (2003), "*Standard Specification for General Requirements for Rolled Structural Steel Bars, Plates, Shapes, and Sheet Piling"*, ASTM A6/A6M-04b, American Society for Testing and Materials, West Conshohocken, PA.

Barth, K.E. et al (2005). *"Evaluation of web compactness limits for singly and doubly symmetric steel I-girders"*, Journal of Constructional Steel Research 61 (2005) 1411–1434.

Dinis, P.B., Camotim, D. (2006). *"On the use of shell finite element analysis to assess the local buckling and post-buckling behavior of cold-formed steel thin-walled members"*, III European Conference on Computational

Mechanics Solids, Structures and Coupled Problems in Engineering C.A. Mota Soares et.al. (eds.) Lisbon, Portugal, 5–8 June 2006.

Earls, C.J. (1999). *"On the inelastic failure of high strength steel I-shaped beams"*, Journal of Constructional Steel Research 49 (1999) 1–24.

Earls, C.J. (2001). *"Constant moment behavior of high-performance steel I-shaped beams"*, Journal of Const. Steel Research 57 (2001) 711–728.

Galambos, T.V., Ketter, R.L. (1959). *"Columns under combined bending and thrust"*, Journal Engineering Mechanics Division, ASCE 1959; 85:1–30.

Galambos, T. (1998). "*Guide to Stability Design Criteria for Metal Structures"*. 5th ed., Wiley, New York, NY, 815-822.

Jung, S., White, D.W. (2006). *"Shear strength of horizontally curved steel I-girders—finite element analysis studies"*, Journal of Constructional Steel Research 62 (2006) 329–342.

Kim, S., Lee, D. (2002). *"Second-order distributed plasticity analysis of space steel frames"*, Engineering Structures 24 (2002) 735–744.

Salmon, C.G., Johnson, J.S. (1996). *"Steel structures: design and behavior: emphasizing load and resistance factor design"* HarperCollins.

Schafer, B.W., Ádány, S. (2006). *"Buckling analysis of cold-formed steel members using CUFSM: conventional and constrained finite strip methods."* Proceedings of the Eighteenth International Specialty Conference on Cold-Formed Steel Structures, Orlando, FL. 39-54.

Schafer, B.W., Seif, M. (2008) *"Cross-section Stability of Structural Steel."* SSRC Annual Stability Conference, April 2008.

Seif, M., Schafer, B.W. (2008). *"Cross-section Stability of Structural Steel."* American Institute of Steel Construction, Progress Report No. 2. AISC Faculty Fellowship, 1 April 2008.

Seif, M., Schafer, B.W. (2009a). *"Elastic buckling finite strip analysis of the AISC sections database and proposed local plate buckling coefficients."* Structures Congress Proceedings, April 2009.

Seif, M., Schafer, B.W. (2009b). *"Cross-section Stability of Structural Steel."* AISC, Progress Report No. 3. AISC Faculty Fellowship, 1 April 2009.

Szalai, J., Papp, F. (2005). *"A new residual stress distribution for hot-rolled I-shaped sections"*, Journal of Const. Steel Research 61 (2005) 845–861.

Shifferaw, Y., and Schafer, B. W. (2008). "*Inelastic bending capacity in cold-formed steel members*." Report to American Iron and Steel Institute – Committee on Specifications, July 2008.

White, D.W. (2008). "*Unified flexural resistance equations for stability design of steel I-section members: Overview.*" ASCE, Journal of Structural Engineering, 134 (9) 1405-1424.